Nano architectured cues as sustainable membranes for ultrafiltration in blood hemodialysis

Muhammad Ali[a], Zaib Jahan[a], Farooq Sher[b,*], Muhammad Bilal Khan Niazi[a], Salik Javed Kakar[c], Saeed Gul[d]

[a]*Department of Chemical Engineering, School of Chemical and Materials Engineering, National University of Sciences and Technology, Islamabad 44000, Pakistan*

[b]*Department of Engineering, School of Science and Technology, Nottingham Trent University, Nottingham NG11 8NS, United Kingdom*

[c]*Department of Healthcare Biotechnology, Atta-Ur-Rahman School of Applied Biosciences, National University of Sciences and Technology, Islamabad 44000, Pakistan*

[d]*Department of Chemical Engineering, University of Engineering and Technology Peshawar, Jamrud Road Peshawar, Khyber Pakhtunkhwa, Pakistan*

*Corresponding author:
Dr. F. Sher
Assistant Professor
Department of Engineering, School of Science and Technology
Nottingham Trent University
Nottingham
NG11 8NS
UK
E-mail address: Farooq.Sher@ntu.ac.uk
Tel.: +44 (0) 115 84 86679

Abstract

Membranes with zeolites are encouraging for performing blood dialysis because zeolites can eliminate uremic toxins through molecular sieving. Although the addition of various pore-gen and adsorbent in the membrane can certainly impact the membrane production along with creatinine adsorption, however, it is not directed which pore-gen along with zeolite leads to better performance. The research was aimed at reducing the adsorption of protein-bound and uremic toxins by using mordenite zeolite as an adsorbent while polyethylene glycol and cellulose acetate as a pore generating agent. Membranes were cast by a phase-inversion technique which is cheap and easy to handle as compared to the electro-spinning technique. Through this strategy, the ability to adsorb creatinine and solute rejection percentage were measured and compared against the pristine PSU, when only PEG was used as a pore-modifier and when PEG along with CA was used as a pore-modifier along with a different concentration of zeolite. The experiments revealed that PEG membranes can give a better solute rejection percentage (93%) but with a low creatinine adsorption capacity that is 7654 µg/g and low bio-compatibility (PRT 392s, HR 0.46%). However, PEG/CA membranes give maximum creatinine adsorption that is 9643 µg/gm and also better bio-compatibility (PRT 490s, HR 0.37%) but with a low BSA rejection (72%) as compared to the pristine PSU and PEG membranes. The present study finds that the concentration of mordenite zeolite affects the membrane performance because its entrapment and large pore size of the membrane decreases solute rejection but increases creatinine uptake level along with the better bio-compatibility.

Keywords: Sustainable hemodialysis membranes; Mordenite Zeolite; Poly-sulfone; Hydrophilicity; Creatinine Adsorption; Uremic Toxins and Biocompatibility.

1 Introduction

Chronic kidney disease (CKD) is one of the major and serious health problems around the globe due to its high deadliness [1]. According to the U.S. Renal Data System, End-stage renal disease (ESRD) has been increased since 2003. According to literature in India and Pakistan, nearly 220,000 to275,000 new patients were reported for renal therapy [2]. The treatment of kidney failure is either a kidney transplant or hemodialysis. The option of kidney transplant is not affordable for every patient and it is a risky procedure too but hemodialysis is an alternative cure and it is a very cost-efficient treatment. In hemodialysis, there is a blood cleaning system along with the hemodialysis-membrane-based dialyzer, which circulates the blood by purifying it coming from the CKD patient [3]. Many clinical up-gradations are required, and some middle-size toxin molecules are still unresolved like indoxyl sulfate, p-cresol and creatinine. Chronic kidney disease is linked with these toxins' development and aggravation.

In hemodialysis, the core component is the membrane. Many researchers had worked on the modification of the membrane by using different polymers along with additives to optimize the rejection capabilities. Different varieties of polymers that were used are cellulose acetate (CA), polysulfone (PSU) [4], polyethersulfone (PES) [5], polymethyl methacrylate (PMMA), polyacrylonitrile (PAN) [6], polyvinyl alcohol (PVA) [7], polylactic acid (PLA), polypropylene (PP), polyamide, chitosan, here every polymer had different abilities in terms of biocompatibility and performance efficiency [8]. PSU is considered the best base polymer because it contains the best mechanical, chemical property and processability. Meanwhile, PSU can remain steady in all disinfection conditions (steam, ethylene oxide, and gamma radiation, etc.) even it is one of the few biomaterials [9]. The PSU membrane becomes the main selection for the clinicians managing

dialysis as from literature shows the best and higher clearance rate of uremic toxins as well in comparison to PES and CA membranes [10]. As the PSU itself is highly hydrophobic in nature that leads to respectively low hemocompatibility. Hence anticoagulants are always used to reduce clot formation during the treatment [11].

Before using the PSU-based hemodialysis membranes, certain modifications are required. To increase the biocompatibility, the researchers have tried to increase the surface modification techniques such as sulfonated hydroxypropyl chitosan (SHPCS) was grafted from PSU membrane material by Schiff-Base reaction [12]. Similarly, the additives can also increase the pore formation and the distribution of the pores are affected [13]. The degradability of the dialysis membrane is affected as between the flowing fluid and the membrane for hemodialysis the shear force can head to loosen the additives from the surface of the membrane [14]. The elution of additives is also affected by the type of dialysis membrane, sterilization method, storage period, and pre-flush methods [15]. Hence optimized handling methods are required to prepare the PSU-based hemodialysis membrane.

The major toxins that are present in the human blood are classified into 3 basic categories depending upon their weight and protein-binding capacity: (1) Small molecular weight water-soluble compounds; (2) Protein-bound compounds and (3) Large sized molecules. The biological effects of protein-bound uremic toxins were also reviewed systematically [16]. To decrease the quantity of protein-bound solutes such as creatinine certain methods are designed which even includes the modification of dialysis procedure such as increasing the K*o*A and Q*d* to increase the

removal or by using sorbents or by just restricting their production [17]. But these methods are expensive.

The hemodialysis method can remove only 30% of the protein-bound toxins because they are bind with albumin. However, it can clear more than 60% of urea & creatinine [18]. The studies suggested that uremic cardiovascular disease and kidney damage are responsible for the most functional deterioration, and it appears that the toxicity of creatinine and supports their roles in vascular and renal disease progression. Because of the activation of the accompaniment of different pathways, it is a major life-threatening complication because it could lead to more adsorption of the proteins during the hemodialysis treatment as PSU is highly hydrophobic in nature [19]. The membrane rejection performance and permeability also deteriorate because of the deposition of the protein on the membrane.

Through the study of the previous literature, it was depicted that the researchers utilized large-sized or rod-shaped adsorbents which lead to decrease surface area and reducing the adsorption of protein-bound toxin [23]. So this study worked on the gap highlighted above by using mordenite zeolite with spherical shape and size which is less than 50 nm that provides more surface area considered as the better adsorbent into the dialysis membrane as it can adsorb more protein-bound toxins onto the porous particle hence also decreasing the risk of cardiovascular disease [21]. Similarly, as a hydrophilic and non-toxic polymer with high portability and anti-interference property to plasma proteins or platelets, PEG [15] and CA [22] used a pore-modifier that can upgrade the hydrophobicity, hemocompatibility, and biocompatibility of PSU.

Hence, the main motivation of this research is to make a composite membrane by using the phase inversion method which is also a cheap method and is associated with mild handling as compared to the hard handling of the electrospinning technique. This strategy directs towards the easy fabrication of the hemodialysis membrane. Similarly, the PEG and CA were used as a pore-modifier to increase the number of pores to reduce the platelets on the membrane surface. In addition, the adsorbent particles named mordenite zeolite of spherical shape were used as an additive in the membrane composition and their size was also smaller than 50 nm hence providing more adsorption sites when incorporated inside the membrane solution. Since it is also a bio-compatible material hence less platelet adhesion would also be obtained. Maximum tests were conducted to find out the performance and biocompatibility of the membrane while changing the concentration of mordenite zeolite. The ability to adsorb creatinine and solute rejection percentage were measured and compared against the pristine PSU, when only PEG was used as a pore-modifier and when PEG along with CA was used as a pore-modifier in terms of urea clearance and BSA rejection and that can also eliminate the protein-bound toxins.

2 Material and methods

2.1 Materials

As a membrane forming basic polymer the PSU with an average molecular weight of 30,000 Da (Sigma Aldrich) was used. The solvent N, N-dimethylacetamide (DMAc) with analytical purity of 99% purchased from Sigma Aldrich. Cellulose Acetate with an average molecular weight of 30,000 Da was purchased from Sigma Aldrich, PEG 400 was taken from Aladdin. Distilled water, n-hexane, and methanol were purchased from Sigma Aldrich and were used as a non-solvent agent. Mordenite zeolite as an adsorbent was purchased from Sigma Aldrich. Experiments were performed using urea with a molecular weight of 60.02 and creatinine were purchased from Sigma

Aldrich. Bovine serum albumin (BSA, purity > 97%) was purchased from Sigma-Aldrich. The anticoagulant sheep whole blood was purchased from Slaughter House.

2.2 Fabrication of pristine PSU and modified membranes

To synthesize the membrane, the PSU flakes were firstly dried in the drying oven at 60 ^{o}C for 24 hours. Then 18 wt.% of the solution was prepared by mixing 18gm of PSU dried flakes as solute into DMAc solvent from which 7 mL of solution was utilized as a base solution. The additive PEG was prepared as 16 % weight into the DMAc solvent and from which 4 mL of solution was mixed with the base solution for pore generation. The CA solution was prepared in 8 wt.% into the DMAc solvent and from which 2 mL was added into the base solution and at the end, the mordenite zeolite was added in different concentrations while the rest was DMAc as a solvent. The solution was stirred for 24 hours at 25 ^{o}C to make the solution homogenous. The complete membrane compositions are given in Table 1.

The solutions were then sonicated for 30 minutes to remove any kind of trapped air bubbles in the solution as these bubbles can deform the membrane surface after casting. The formulated solution was then cast by using doctors' blade on the glass slab by pouring that much solution to make the membrane to the size of 0.00146 m^2 with a thickness of 200 µm. After evaporating for 30 to 45 seconds, it is then immersed in the distilled water coagulation bath for 24 hours then in an n-hexane and methanol coagulation bath for 2 hours respectively to complete the phase inversion process as shown in Fig. 1. The side facing the non-solvent is the reactive side of the membrane. The distilled water helps in solidifying the membrane while n-hexane and methanol act as a non-solvent agent. Then the membrane is placed in a neat place for 24 hours for drying.

2.3 Membranes characterization

In SEM model JSM 6490A, JEOL analysis, the dried samples react with the electron beams when the voltage was kept at the 10 kV and produced surface and cross-sectional morphology of the membranes and their relative composition at various magnifications [23]. Dried samples were sputtered with liquid nitrogen to obtain clear cross-sectional morphology. In AFM JSPM-5200, three-dimensional topographies were obtained for the image down to the sub-nanometer range by using the high-resolution technique [24]. The AFM non-contact mode was utilized by using a silicon nitrate tip. AFM software program determined the roughness of the sample membranes from AFM 3D micrographs. MID-IR instrument was used for the chemical composition measurements of the modified membranes. The transmission method was used to find the FTIR and the range was kept at the resolution of the 4 cm^{-1} and spectrometer range 400-4000 cm^{-1}. Infrared radiations were used to study various functional organic groups in the membrane samples [24]. All characterization techniques were performed on the side of the membrane facing the non-solvent during the membrane fabrication.

2.4 Hydrophilicity tests

2.4.1 Porosity

The 1×1 cm^2 area of the membrane was oven-dried and weighed and then immersed in distilled water for 24 hours and weighed again. The membrane porosity can be obtained by using Eq. (1). W is the weight of the wet and dry membranes (grams), $\boldsymbol{\rho}_w$ is the density of the pure water (gm/cm^3) and $\boldsymbol{\rho}_p$ is the density of polymer (gm/cm^3), respectively [25].

$$\text{Porosity } (€) = \frac{\dfrac{W_{wet} - W_{dry}}{\rho_w}}{\dfrac{W_{wet} - W_{dry}}{\rho_W} + \dfrac{W_{dry}}{\rho_p}} \tag{1}$$

2.4.2 Degree of swelling

Membranes were pre-heated at 60 ^{o}C for 12 hours and weighted (W_{dry}) in grams. The soaked membranes were removed from the water after 24 hours and weighed again (W_{wet}) in grams [26]. The measurement was made at 5 different positions and the average was taken [26]. Then from Eq. (2).

$$\text{Water Uptake (\%)} = \frac{W_{wet} - W_{dry}}{W_{dry}} \times 100 \qquad (2)$$

2.4.3 Contact angle measurement

Contact angle system OCA (Data physics, USA) was used for this experimentation. The sessile drop method was used to measure the stable contact angle. Synthesized membrane area 1×5 cm^2 was taken and attached to the glass slide. Distilled water was poured on the sample by using a micro syringe with a constant dosing rate of 0.2 µL The water drop angle was recorded and measured on the surface three times for average angle [27].

2.5 Performance tests of membranes

2.5.1 Tensile strength test

The ultimate tensile strength experiment was carried out with the help of Shimadzu; AGS-X series of 50KN. ASTM-standard D 8802-02 was at a strain rate of 0.5mm/min, the stress-strain behaviour was observed for all samples[28].

2.5.2 Water flux and permeability

Water flux, as well as permeability experiments were performed in dead-end filtration cell with 2 bar pressure maintained by nitrogen gas [29]. 0.00146 m^2 area of the membrane sample was used and the permeate was calculated after every 10 minutes and after 1 hour 40 minutes the flux became constant. The pure water flux and permeability were then calculated by using Eq. (3) and

Eq. (4) [25]. Where J is the flux in L/m^2 h. V is the volume of the permeated water in Litres. T is the time in hours. A represents the total area of the membrane in cm^2.

$$J = \frac{V}{A \times T} \tag{3}$$

$$\text{Permeability} = \frac{\text{Flux}}{\text{pressure}} \tag{4}$$

2.5.3 BSA rejection percentage and urea clearance

After feeding 1 mg/mL BSA solution and 1mg/mL urea solution the permeate obtained after applying 2.5 bar pressure was observed under the (Shidmazu UV 1240) spectrophotometer at a wavelength of 278 nm and 190 nm. The BSA rejection percentage and urea clearance percentage were then calculated by Eq. (5) and Eq. (6) [29]. Where Cp (gm/L)and Cr (gm/L) are concentrations of permeate and retentate , respectively [29]. Moreover, Ci (gm/L) and Cf (gm/L) are initial and final concentrations at time t, respectively [29].

$$\text{BSA Rejection (\%)} = 1 - \frac{C_p}{C_r} \times 100 \tag{5}$$

$$\text{Solute Clearance (\%)} = \frac{C_i - C_f}{C_i} \times 100 \tag{6}$$

2.5.4 Creatinine adsorption capacity

The round modified membranes with 10mm in diameter were placed in a syringe filter cartridge (EMD Millipore, CA) to measure the creatinine adsorption capacity [21]. Then, a 400 mmol/L creatinine solution was added into the inlet of the cartridge that flows through the membrane at 2.5 bar pressure. Finally, the solution collected at the outlet were measured by (Shidmazu UV 1240) UV absorption spectra at a wavelength of 190 nm. Each type of membrane was tested thricely.

2.6 Hemocompatibility study of membranes

2.6.1 Static Platelet adhesion test

Platelet attachment is observed by the SEM technique. Firstly, the plasma-rich-plasma (PRP) was obtained when 10 mL of anticoagulant whole blood was centrifuged at 1000 rpm for ten minutes. 1×1 cm^2 membrane samples were washed with the phosphate buffer solution (PBS). 100 µL PRP was inserted on the samples in 24-well cultural plate. After incubation for 2 hours at 37 ^oC for the removal of unstable platelets, the samples were washed thrice. The membranes were then immersed in 2.5 wt% glutaraldehyde solution which was used to fasten the absorbed protein on the membrane surface for 24 hours. Further drying was done with the graded ethanol of compositions 50, 75, 85, 95 and 100% [30].

2.6.2 Hemolysis Ratio measurements

1×1 cm^2 membranes samples were washed thrice with the 0.9 wt% of the NaCl solution for ten minutes in sequence [12]. At 37 ^oC in a water bath for one hour the samples were kept immersed in the NaCl solution and whole blood of 200 µL was added to the membrane samples. Then this solution was centrifuged for 10 minutes at 1500 rpm and top layer absorbance was measured using 545 nm by (Shidmazu UV 1240) UV spectrophotometer. The ratio was calculated using Eq. (7) in which HP and HN represent absorption value of negative reference and absorption value of the positive reference, respectively. HS represents the absorption value of membrane samples [31].

$$\mathrm{HR} = \frac{\mathrm{HS} - \mathrm{HN}}{\mathrm{HP} - \mathrm{HN}} \tag{7}$$

2.6.3 Thrombus formation measurements

Membrane samples of 1×1 cm^2 were immersed in the 1.5 mL whole blood and incubated in 5% of CO_2 for 2 hours at 37 $^{\circ}C$. PBS was used after the incubation to wash the samples. The in vitro thrombus formation on the membrane surface was measured by the graded ethanol and critical

point drying [32]. The Eq. (8) is used in which DT is the degree of thrombus; W_t (gm) and W_d (gm) represent the weight of blood-coagulated membrane and weight of the dry membrane.

$$DT = \frac{W_t - W_d}{W_d} \tag{8}$$

2.6.4 Plasma clotting time measurements

The plasma poor plasma (PPP) was obtained when anticoagulant 10 mL blood was centrifuged at 3000 rpm for 15 minutes. 200 µL of PPP was poured on the 1×1 cm^2 membrane samples and the cultural plate was incubated in a water bath for 10 minutes at 37 ^oC. Then 100 µL of the 0.025 mol/L $CaCl_2$ solution was added to the samples. The mixture was stirred until any thread formed, the time consumed was recorded [33].

3 Results and discussion

3.1 Morphology and chemistry of the membranes

SEM is the analytical technique that explains the surface and cross-sectional morphology of the membrane. It explains the effect on the PSU membrane by adding CA and PEG as a pore-generating agent. All the membranes SEM comparison images are shown in Fig. 2. The surface morphology revealed that when the additives were added the surface contains more non-uniform pores and long finger-like structural pores along with sub pores are formed in the cross-section [9]. With the addition of mordenite, the surface and cross-sectional morphology changed as the zeolite nanoparticles can be seen in the SEM images properly dispersed inside the cross-section but also on the surface of the membrane. It can also be seen that as the concentration of mordenite zeolite increased from 0.18 to 0.98 gm the pores become smaller making the membrane denser again which also affects the selectivity of the membrane for toxin removal.

The surface image of the pristine PSU membrane showed that pores of the top layer were very small that they cannot be shown by SEM hence the membrane surface is highly dense, whilst the PEG/CA and PEG membranes showed pores and gap structure on the membrane surface. When PEG and CA were added to the membrane solution, the casted membrane surface showed more non-uniform pores with large size along with macro voids as shown in Fig. 2(b) and (c) in comparison to the pristine PSU but at the bottom, the pores were smaller or of the same size of pristine PSU when inspected at the cross-sectional image Fig. 2(b) and (c). With the addition of only PEG, the membrane surface pores were of smaller and equal size up till the bottom of the membrane as shown in Fig. 2(d), (e), and (f). With the addition of PEG, the fingers length increased in the cross-section of the membrane as shown in Fig 2(d, e, f). However, with the addition of PEG along with CA, the width of the fingers also increased as shown in Fig. 2. The integral membrane surface roughness became very rough, even though there were some small circular structural pores on the skin of the membrane after the addition of additives. Less surface roughness can also prevent the adsorption of significant quantities of protein [34].

The surface chemical composition of modified membranes was determined by FT-IR spectroscopy and is shown in Fig. 3. In cases of PEG-1, PEG-3, PEG-5 membranes, the bands at 1244 cm^{-1} were due to the C-O-C bond that shows the existence of PEG additive. At near 3023 cm^{-1} the slight increase in the band was due to the C-H bond that also showed the presence of PEG. In all the spectra, the existence of C-O at 1478 $cm^{-1}$and C-O-C ether group at 1198 cm^{-1} shows the presence of PEG due to asymmetric stretching in all the PEG blend membranes. Meanwhile, when PEG along with CA act as a pore-modifier for PEG/CA-1, PEG/CA-3, PEG/CA-5 membranes at 1500 cm^{-1} the increase in the band was due to the C-O bond this is because of the presence of CA.

However, the sharp band at 1244 cm^{-1} was due to the C-O-C bond of the PEG additive. These C-O-C and C-O bonds not shown much stretching due to their constant wt%. The R-SO_2 bonds near 1100 cm^{-1} showed a proper dispersion of mordenite zeolite in the membrane structure and the slight stretching in the band was due to the change in its concentration. The PSU characteristic bands were around 1149 and 1168 cm^{-1} (SO_2 symmetrical stretching), 1244 cm^{-1} (aryl-O-aryl C–O stretching), 1582 cm^{-1} (SO_2 asymmetric stretching), 1677 cm^{-1} (asymmetric–CH_3), and 2151 cm^{-1} (C=C) [35].

The AFM explains the surface topography of the membrane surface as shown in Fig. 4. All the samples were examined under AFM in tapping mode. 3D AFM images of the top surface of all the membranes with a scanning area of (10×10 µm) were taken as 3D images can identify the surface roughness and smoothness. The dark regions showed depths and the light regions defined the heights on the surface topography [36]. The optimum surface roughness is required to obtain better biocompatibility. Fig. 4 shows that the pristine PSU membrane surface was smooth enough but when the PEG, CA, and mordenite zeolite were added the membrane became highly rough because of the pore and the macro void formation, and as the amount of mordenite zeolite was increased the membrane roughness started decreasing because of the presences of mordenite zeolite because the void spaces between the pores started decreasing hence making the membrane less smooth.

Fig. 4(a) revealed the pristine PSU was highly smooth but when CA along with PEG were added as an additive, the membrane became highly rough Fig. 4(b, c). When only PEG acted as pore-modifier the membrane showed less roughness in comparison to PEG/CA membranes as shown in Fig. 4(d, e, f). The lesser the roughness, the better be the biocompatibility results because of the

low adsorption of protein on its surface. It would also give good fluxes and most importantly low fouling rates [37]. From Fig. 4 the AFM images justify the statement that PEG membranes show optimum smoothness than PEG/CA and PSU membranes.

3.2 Membrane performance evaluation for dialysis

3.2.1. Evaluation of hydrophilicity level of the membranes

The increment in the contact angle is due to the higher densities and compaction of the synthesized membranes. As shown in Fig. 5 (b) that pristine PSU is highly hydrophobic in nature because the presence of a dense surface giving an angle of $87^{\circ}\pm5^{\circ}$ that make it less promising for the hemodialysis process. However, when PEG along with CA used as a pore-modifier, the minimum angle reached $48.1^{\circ}\pm5^{\circ}$ for PEG/CA-1 membrane, this is just because the formation of the pore and macro voids on the surface of the membrane and sub pores were also increased in the finger-like structure of the membrane that can be seen by SEM images. However, when only PEG acted as a pore-generating agent, the minimum angle obtained was $58.6^{\circ}\pm5^{\circ}$ for the PEG-5 membrane. Fig. 5 (b) justifies that now the modified membranes are hydrophilic in nature that is the main requirement for the optimum hemodialysis process. A contact angle lesser than 60° is considered as hydrophilic and more than or equal or closer to 90° is considered hydrophobic in nature [5]. When the membrane is more hydrophilic best hemocompatibility results could be obtained [12]. The PEG/CA membranes are more hydrophilic in nature than pristine PSU and PEG membranes. Because of the penetration of the water into the pores of the membrane due to the capillary tube affect the porosity also plays an important role in the contact angle measurement [5].

When the porosity and the pore size distribution are changed, it causes a major effect on the permeability of water, uremic toxin clearance, and protein adsorption and rejection clearance.

When PEG with CA and mordenite zeolite were added to the PSU solution, the porosity percentage increased abruptly as compare to the pristine PSU this was due to the increase in the number and size of pores on the surface but also the sub pores in the finger-like structure of the membrane that can be seen in SEM imaging Fig. 2. The porosity of PEG/CA-1 was 93.5%±5%. However, for PEG/CA-3 and PEG/CA-5, the porosity was 79.6%±5% and 72.1%±5% respectively. Fig. 5 (a) showed the trend that when the concentration of zeolite increased it blocked and captured the void spaces between the pores resulting in decreasing in the porosity. However, when only PEG as an additive was added the porosity trend increased as with the increase in the concentration of mordenite zeolite. and the maximum porosity obtained for the PEG-5 membrane was 79.2%±5% as shown in Fig. 5 (a). This trend showed that as the concentration of mordenite zeolite increased, the surface area of the membrane morphology also increased hence resulting in increased membrane porosity.

The hydrophilicity and hydrophobicity of the membrane can also be determined by the swelling percentage test. High water absorption means that the membrane is hydrophilic in nature [9]. Fig. 5 (a) elaborates the trend in the results. The pristine PSU membrane showed very less water absorption as the surface of the membrane was very dense containing very little and no pores. But when the PEG along with CA and mordenite zeolite as an additive were added the water absorption increased to a very high extent because of the increase in porosity justified by Fig. 5(a). As shown in Fig. 5(a), the maximum percentage was obtained for the PEG/CA-1 membrane was 1189% ± 10% this was just because of an increase in the number and size of the pores on the surface but also in the cross-section of the membrane that can be seen in the SEM image Fig. 2. Hence, the PEG/CA-1 membrane is highly hydrophilic that can absorb maximum water. On the other hand,

when only PEG acts as a pore-modifier the trend started increasing with the increase in the concentration of the mordenite zeolite as shown in Fig. 5 (a) this happened because zeolite provides more surface area when incorporated in the membrane. PEG-5 membrane was highly hydrophilic in nature giving the percentage of 666% ± 10%.

3.2.2. Effect of the toughness of membranes on hydrophilicity

The addition of hydrophilic elements like PEG and CA can also affect the mechanical properties of the membranes that can also be compared by their morphology. Fig. 6 represents that the pristine PSU membrane showed the highest tensile stress of 30.76 MPa. Because the pristine PSU membrane contains a dense structure as shown in SEM image Fig. 2, the high tensile stress and strain curve justify that it was very dense and contained fewer pores on the surface, as well as short-sized fingers in the cross-section of the membrane, were present. However, when the additives like PEG along with CA were added to the membrane the tensile stress decreased abruptly to 9.98 MPa of PEG/CA-3 membrane, due to the less density, polymer packing and favourable interfacial adhesion.

However, with the addition of PEG, the tensile stress was 25.8 MPa for the PEG-1 membrane which was still lesser than pristine PSU. The mechanical properties decrease when the structure changes to more porosity and hydrophilicity [38]. Further, when mordenite zeolite concentration increased in PEG/CA membranes it increased the stress as well as strain than the previous compositions showing that the void spaces between the pores now start blocking hence making the membrane denser again. Similarly, because of the addition of the pore-modifier, the elongation rate also increased as cross-sectional morphology also influenced mechanical properties justifying

that the membrane contained more pores, and sub pores were also produced in the fingers in the cross-section of the membrane as shown in Fig. 2.

3.2.3. Water flux and permeability of the membranes

The efficiency evaluation of the modified and pristine PSU membrane, pure water permeability test was performed. The distilled water as a solvent was used to determine the behaviour of the membranes. The flux was then calculated and then the graph was plotted as shown in Fig. 7. When the additives were added, the void spaces, pore sizes and sub pores the permeability and flux of the modified membrane were increased [39]. The increase in hydrophilicity and porosity enhances the selectivity of the membrane to pass water molecules through it. In the permeability test, the dead-end filtration cell was utilized. The flux and permeance were measured after every 10 minutes, the final measurements were obtained after 80 minutes where all the membranes gave constant fluxes at a constant pressure of 2 bar. The pure water flux that was obtained for pristine PSU was very low 17.91±2 L/m^2 h which was extremely less than the modified membrane. This behaviour occurs because of the less bonding interaction and also due to the dense surface morphology (fewer and small surface pores) of the membrane).

The PEG/CA-1 membrane showed maximum flux and permeability because of its less contact angle and high porosity which was 45.5±2 L/m^2 h and 22.2±5 L/m^2 h bar respectively. As shown in Fig. 7 that as the concentration of the mordenite zeolite increased it decreased the flux because the void spaces between the pores start blocking the membrane and making the membrane denser. Hemodialysis requires moderate water flux so that less water will be lost from the blood during the dialysis process so from the graph PEG/CA-3 membrane showed moderate flux and permeability that was 41.224±2 L/m^2 h and 20.612±5 L/m^2 h bar respectively as shown in Fig. 7

[9]. Similarly, when only PEG as a pore-modifier was added, the trend increased gradually as shown in Fig. 7 so PEG-3 can be considered as the better membrane with moderate 24.901±2 L/m^2 h of flux and 12.445±5 L/m^2 h bar respectively of permeability.

3.2.4. Solute rejection and clearance percentage analysis

The albumin loss can be controlled by the membrane morphology and composition to justify this BSA with a molecular weight of 67 kDa was used to determine the solute rejection percentage [9]. Some membranes can have poor water flux but BSA retention should be higher than 75% for good dialysis treatment. For to characterize the loss of BSA during the 6 h dialysis simulation is used to determine the loss of beneficial proteins [40]. Fig. 8 showed that pristine PSU cannot reject BSA because of the dense surface of the membrane. Meanwhile, the maximum rejection of the BSA was obtained in the PEG/CA-1 membrane that was 83.21%±5% because of the irregular porous surface and also the sub pores in the fingers of the membrane. However, when only PEG as a pore-modifier was added, the BSA rejection increased to 93.5%±5% in the PEG-5 membrane as shown in Fig. 8. This difference in the membranes for BSA rejection justifies that optimization is required in the pore size of the PEG/CA membranes to increase the BSA rejections to a maximum percentage. All PSU family polymers need very optimized handling to make optimized pore size [41].

As the uremic toxins also contain urea which is important to remove from the blood during the dialysis process. Fig. 8 shows that PEG/CA-1 membrane gave clearance of 72%±5%, which was more than the pristine PSU membrane with the increase in water flux. The urea clearance then decreased after that due to denser membranes because of the presence of high concentrations of mordenite zeolite and blockage of the pores with urea molecules coming from different directions.

For PLA membrane the maximum urea clearance was over 70% [42]. From Fig. 8 when only PEG acts as an additive, the urea clearance reached 93%±5%. In the literature, when using CA as a base polymer the maximum clearance for the urea was 80.39%±5%. [43]. So, with the addition of only PEG as a pore-modifier, the pores were uniformly scattered throughout the membrane, hence it gives maximum urea clearance this statement can also be justified by the SEM morphology Fig. 2(d, e, f). But here with the increase in the concentration of mordenite zeolite the urea clearance also increases because the mordenite zeolite provides more surface area along with the macro-void formation with the pores.

3.2.5. Creatinine adsorption capacity by composite membranes

Creatinine is a uremic toxin formed in the muscles by the degradation of creatine phosphate. In relation to the degree of creatinine absorption, the size and shape of zeolite particles can theoretically affect the efficiency of the membranes. The effect of the concentration of mordenite zeolite inside the membrane on the creatinine uptake level was observed. The mordenite zeolite was selected as it has a spherical shape and the size of the particle is 48 nm in diameter that will provide more adsorption sites for the adsorption of creatinine. From the literature, the spherical-shaped particles work better inside the membranes than rod-shaped zeolite [44]. As the powdered zeolite can adsorb more creatinine rather than when it was incorporated inside the membrane this is just because 1/3 of the adsorption site of the nanoparticle was blocked when particles were incorporated on the surface but also inside the fingers of the membranes [21].

From Fig. 9, the trend explains that as the concentration of the mordenite zeolite increases in the composition of the membranes the adsorption capacity of the creatinine also increased hence making the membrane more suitable for the removal of protein-bound toxins. Hence the PEG/CA-

5 with 9643 µg/gm can adsorb maximum creatinine compared to the PEG-5 membrane with 7654 µg/g as shown in Fig. 9. This is because the pore size is small and are less in number so when the nano-particles were incorporated the reactive sites are masked in the membrane. As the shape and size of the nanoparticle integrated inside the membrane had a great effect on the creatinine adsorption as in literature while using PAN as a polymer along with the rod-shaped zeolite particle the creatinine adsorption was 7000 µg/gm [21].

3.3 Biocompatibility evaluation of membranes

The objective of this research was to reduce the number of platelets on the surface of the membrane. SEM photographs have been utilized to observe the platelet adhesion behaviour over the skin of the membrane. As shown in Fig. 10, the overall surface of the pristine PSU membrane had evident platelet adsorption. In addition, all reticulate pseudopodia structures displayed adhesion of platelets, suggesting activation of platelets. But the involvement of ether bond in PEG by hydrogen bonding can be closely coupled with water molecules that form a hydration layer (physical and energetic barrier) near the surface with the addition of PEG/CA and mordenite zeolite to keep the bio components from adsorbing the polymer surface as also shown in Fig. 3 of FT-IR spectrum [45]. From the literature, a large number of platelets aggregated on the hydrophobic membrane surfaces such as pristine PSU or PLA membranes [44]. Therefore, the PEG/CA-1 layer, expressed on the membrane surface by PEG chains, enables the best anti-protein surface that effectively inhibits platelet accumulation. It can be assumed that this strong performance of anti-surface assimilation can be sustained for a long time rather than steadily decreasing over time since PEG and PSU are covalently bonded with each other. Although the platelet cannot adequately aggregate on membrane surface due to the larger pore sizes, hence less platelet adhesion can be observed in Fig. 10(b) as compared to Fig. 10(c, d).

The thrombus formation was being examined by using the whole blood. In the formulation of the blood-contacting membrane, the main obstacle is self-induced thrombosis [45]. Therefore, as the pristine PSU membrane was highly hydrophobic in nature due to less hydrogen bonding justified by the contact angle measurement from Fig. 5(b), hence it contained the highest thrombus formation value which was 9%±0.3% as the platelets were highly aggregated on the surface of the membrane. However, with the addition of additives, the thrombus formation decreases. From Fig. 11(a), when PEG along with CA act as a pore-modifier the minimum value was obtained for PEG/CA-1 membrane which was 5%±0.3%. When only PEG acts as a pore-modifier the minimum value of thrombus formation was 5.06%±0.3% for PEG-1 membrane. However, from Fig. 11(a) the trend explains that with the increase in the concentration of the mordenite zeolite the thrombus formation also increased slightly. So, the more accumulation of the platelets on the surface of the membrane occurs the more thrombus formation value is obtained.

Because of the association of erythrocytes with the membranes, erythrocytes can burst and let out hemoglobin (known as hemolysis). To assess the degree of damage to the erythrocytes by the dialysis membranes, HR is then used. The ASTMF-756-08 finds that HR below 5% is considered to be harmless. In comparison to all of the polymers, the pristine PSU membrane gave 0.55% ± 0.03% however with the addition of PEG along with CA the value decreased to 0.37% ± 0.03% for PEG/CA-1 membrane which was extremely lesser than 5% hence proving that the membranes have excellent hydrophilicity, electronegativity and anti hemolytic activity justified by the contact angle. Similarly, from Fig. 11(a), when only PEG acts as a pore-modifier the values were 0.46%± 0.03% for PEG-1 membrane which was lesser than 5% and still lesser than in the literature as it

reduces the damage to erythrocytes with addition to blood clotting and platelet adhesion prevention [45]. The slight increase in the trend can be seen due to the decreased porosity and contact angle measurement as shown in Fig. 5(b) [41]. Certain polymers give certain hemolysis ratios like when PSF/PSF-*g*-TPG is used the HR was 0.53% [11].

The clotting time and the presence and absence of clotting factor can be determined by PRT [31]. When the blood meets activated factor VIII and the presence of Ca^{-2}, fibrous proteins cross-linked with each other lead to the formation of thrombus. Thrombus formation time depends upon the hydrophilicity and presence of hydroxyl, carboxyl groups [32]. The PRT of the pristine PSU membrane was 321s ±20s as shown in Fig. 11(b). As the thrombus formation is greatly reliant on the hydrophilicity of the membrane. PEG is considered as a hydrophilic and biocompatible material which is the main cause of increment in the PRT because the functional groups increase plasma slowly forms the adsorptive layer on the surface resulting in the enhancement of the biocompatibility. So with the addition of the additive (PEG), the PRT increased to 392s±20s and when (CA along with PEG) was added the PRT increased to 490s ±20s which proved that the activation of fibrinogen on PEG/CA-1 membranes was repressed, due to the improvement of membrane hydrophilicity [46]. But due to the increase in the concentration of the mordenite zeolite, the PRT starts decreasing as the membrane surface starts becoming hydrophobic in nature Fig. 11 (b) justifies the statement.

4 Conclusion

Fabrication and characterization of Poly-sulfone hemodialysis membranes with better biocompatibility and uremic toxin clearance were obtained by the addition of hydrophilic compounds like PEG and CA. The spherical structure and uniform-sized zeolite particles named

mordenite zeolite adsorb more medium toxins hence provided the maximum reactive site while it was incorporated in the membrane. When PEG along with the CA was added in membrane solution, membrane became more hydrophilic such that 9643 µg/gm of creatinine were adsorbed along with plasma recalcification time of 490s along with the lowest hemolysis ratio that is 0.37% but the solute rejection was only 83% as compared to PEG membranes. However, when only PEG was added to the membrane solution, creatinine adsorption was 7654 µg/g with less PRT 392s but the maximum solute rejection obtained was 93%. The modified membranes also showed excellent stability in water. Medium toxins like indoxyl sulfate and p-cresol adsorption and adsorption effect on pH and salts tests can be performed to justify that with the smaller sized zeolite particle more amount of medium toxins can be adsorbed in the membrane.

Acknowledgement

The authors are grateful for the financial supports from the Engineering and Physical Sciences Research Council (EPSRC) UK and from the Higher Education Commission of Pakistan to carry on this research.

References

[1] S. K. Verma, A. Modi, A. K. Singh, R. Teotia, and J. Bellare, *"Improved hemodialysis with hemocompatible polyethersulfone hollow fiber membranes: In vitro performance,"* Journal of Biomedicals Materials Research - Part B Applied Biomaterials, vol. 106, no. **3**, pp. 1286–1298, 2018.

[2] V. Jha, *"Current status of end-stage renal disease care in India and Pakistan,"* Kidney International Supplements, vol. 3, no. **2**, pp. 157–160, 2013.

[3] R. Sinnakirouchenan and J. L. Holley, *"Peritoneal dialysis versus hemodialysis: Risks, benefits, and access issues,"* Advances in Chronic Kidney Diseases, vol. 18, no. **6**, pp. 428–432, 2011.

[4] H. Wang *et al.*, *"Enhanced hemocompatibility of flat and hollow fiber membranes via a heparin free surface crosslinking strategy,"* Reactive and Functional Polymer, vol. 124, no. December 2017, pp. 104–114, 2018.

[5] M. Irfan, A. Idris, N. M. Yusof, N. F. M. Khairuddin, and H. Akhmal, *"Surface modification and performance enhancement of nano-hybrid f-MWCNT/PVP90/PES hemodialysis membranes,"* Journal of Membrane Sciences, vol. 467, pp. 73–84, 2014.

[6] L. Ma *et al.*, *"Hemocompatible poly(lactic acid) membranes prepared by immobilizing carboxylated graphene oxide: Via mussel-inspired method for hemodialysis,"* RSC Advances, vol. 8, no. **1**, pp. 153–161, 2018.

[7] X. Yu *et al.*, *"High performance thin-film nanofibrous composite hemodialysis membranes with efficient middle-molecule uremic toxin removal,"* Journal of Membrane Sciences, vol. 523, pp. 173–184, 2017.

[8] F. Galiano, K. Briceño, T. Marino, A. Molino, K. V. Christensen, and A. Figoli, *"Advances in biopolymer-based membrane preparation and applications,"* Journal of Membrane Sciences, vol. 564, no. May, pp. 562–586, 2018.

[9] D. Zhong, Z. Wang, J. Zhou, and Y. Wang, *"Additive-free preparation of hemodialysis membranes from block copolymers of polysulfone and polyethylene glycol,"* Journal of Membrane Sciences, vol. 618, no. August 2020, p. 118690, 2021.

[10] O. E. M. ter Beek, D. Pavlenko, and D. Stamatialis, *"Hollow fiber membranes for long-term hemodialysis based on polyethersulfone-SlipSkin^{TM} polymer blends,"* Journal of Membrane Sciences, vol. 604, no. January, p. 118068, 2020.

[11] G. J. Dahe, R. S. Teotia, S. S. Kadam, and J. R. Bellare, *"The biocompatibility and separation performance of antioxidative polysulfone/vitamin E TPGS composite hollow fiber membranes,"* Biomaterials, vol. 32, no. **2**, pp. 352–365, 2011.

[12] T. M. Liu, J. J. Xu, and Y. R. Qiu, *"A novel kind of polysulfone material with excellent biocompatibility modified by the sulfonated hydroxypropyl chitosan,"* Materials Science and Engineering C, vol. 79, pp. 570–580, 2017.

[13] E. Salehi and S. S. Madaeni, *"Influence of poly(ethylene glycol) as pore-generator on morphology and performance of chitosan/poly(vinyl alcohol) membrane adsorbents,"* Applied Surface Sciences, vol. 288, pp. 537–541, 2014.

[14] K. Namekawa, M. Matsuda, M. Fukuda, A. Kaneko, and K. Sakai, *"Poly(N-vinyl-2-pyrrolidone) elution from polysulfone dialysis membranes by varying solvent and wall shear stress,"* Journal of Artificial Organs, vol. 15, no. **2**, pp. 185–192, 2012.

[15] M. Kohlová, C. G. Amorim, A. da Nova Araújo, A. Santos-Silva, P. Solich, and M. C. B. S. M. Montenegro, *"In vitro assessment of polyethylene glycol and polyvinylpyrrolidone as*

hydrophilic additives on bioseparation by polysulfone membranes," Journal of Materials Science, vol. 55, no. **3**, pp. 1292–1307, 2020.

[16] R. Vanholder, E. Schepers, A. Pletinck, E. V. Nagler, and G. Glorieux, *"The uremic toxicity of indoxyl sulfate and p-cresyl sulfate: A systematic review,"* Journal of the American Society of Nephrology, vol. 25, no. **9**, pp. 1897–1907, 2014.

[17] O. Stress, "Hemodialysis Impairs Endothelial Function," pp. 1002–1007, 2015.

[18] Y. Itoh, A. Ezawa, K. Kikuchi, Y. Tsuruta, and T. Niwa, *"Protein-bound uremic toxins in hemodialysis patients measured by liquid chromatography/tandem mass spectrometry and their effects on endothelial ROS production,"* Analytical and Bioanalytical Chemistry, vol. 403, no. **7**, pp. 1841–1850, 2012.

[19] M. Ji, X. Chen, J. Luo, and Y. Wan, *"Improved blood compatibility of polysulfone membrane by anticoagulant protein immobilization,"* Colloids Surfaces B Biointerfaces, vol. 175, no. December 2018, pp. 586–595, 2019.

[20] M. Tijink *et al.*, *"Development of novel membranes for blood purification therapies based on copolymers of N-vinylpyrrolidone and n-butylmethacrylate,"* Journal of Materials Chemistry B, vol. 1, no. **44**, pp. 6066–6077, 2013.

[21] L. Lu, C. Chen, C. Samarasekera, and J. T. W. Yeow, *"Influence of zeolite shape and particle size on their capacity to adsorb uremic toxin as powders and as fillers in membranes,"* Journal of Biomedical Materials Research - Part B Applied Biomaterials, vol. 105, no. **6**, pp. 1594–1601, 2017.

[22] A. Idris and L. K. Yet, *"The effect of different molecular weight PEG additives on cellulose acetate asymmetric dialysis membrane performance,"* Journal of Membrane Sciences, vol. 280, no. **1**–**2**, pp. 920–927, 2006.

[23] Q. Chen, Y. He, Y. Zhao, and L. Chen, *"Tannic acid and Poly(N-acryloyl morpholine) layer-by-layer built hemodialysis membrane surface for intervening oxidative stress integrated with high biocompatibility and dialysis performance,"* Journal of Membrane Sciences, vol. 621, p. 118896, 2021.

[24] O. T. Mahlangu, R. Nackaerts, J. M. Thwala, B. B. Mamba, and A. R. D. Verliefde, *"Hydrophilic fouling-resistant GO-ZnO/PES membranes for wastewater reclamation,"* Journal of Membrane Sciences, vol. 524, no. November 2016, pp. 43–55, 2017.

[25] H. Waheed, F. T. Minhas, and A. Hussain, *"Cellulose acetate/sericin blend membranes for use in dialysis,"* Polymer Bulletin, vol. 75, no. **9**, pp. 3935–3950, 2018.

[26] D. Zhong, Z. Wang, Q. Lan, and Y. Wang, *"Selective swelling of block copolymer ultrafiltration membranes for enhanced water permeability and fouling resistance,"* Journal of Membrane Sciences, vol. 558, no. April, pp. 106–112, 2018.

[27] H. Waheed and A. Hussain, *"Preparation and Solvents Effect Study of Asymmetric Cellulose Acetated/Polyethyleneimine Blended Membranes for Dialysis Application,"* International Journal of Health and Medicines, vol. 2, no. **4**, p. 5, 2017.

[28] A. Bernal-Ballén, I. Kuritka, and P. Saha, *"Preparation and Characterization of a Bioartificial Polymeric Material: Bilayer of Cellulose Acetate-PVA,"* International Journal of Polymeric Sciences, vol. 2016, 2016.

[29] L. Zhu, F. Liu, X. Yu, A. Gao, and L. Xue, *"Surface zwitterionization of hemocompatible poly (lactic acid) membranes for hemodia fi ltration,"* Journal of Membrane Sciences, vol. 475, pp. 469–479, 2015.

[30] S. Senthilkumar, S. Rajesh, A. Jayalakshmi, and D. Mohan, *"Biocompatibility studies of polyacrylonitrile membranes modi fi ed with carboxylated polyetherimide ☆,"* Materials

Science and Engineering C, vol. 33, no. **7**, pp. 3615–3626, 2013.

[31] A. Gao, F. Liu, and L. Xue, *"Preparation and evaluation of heparin-immobilized poly (lactic acid) (PLA) membrane for hemodialysis,"* Journal of Membrane Sciences, vol. 452, pp. 390–399, 2014.

[32] X. Yu, Y. Zhu, C. Cheng, T. Zhang, X. Wang, and B. S. Hsiao, *"Novel thin-film nanofibrous composite membranes containing directional toxin transport nanochannels for efficient and safe hemodialysis application,"* Journal of Membrane Sciences, vol. 582, no. April, pp. 151–163, 2019.

[33] A. Mollahosseini, A. Abdelrasoul, and A. Shoker, *"A critical review of recent advances in hemodialysis membranes hemocompatibility and guidelines for future development,"* Materials Chemistry and Physics, vol. 248, no. March, p. 122911, 2020.

[34] R. Teotia, S. K. Verma, D. Kalita, A. K. Singh, G. Dahe, and J. Bellare, *"Porosity and compatibility of novel polysulfone-/vitamin E-TPGS-grafted composite membrane,"* Journal of Materials. Science, vol. 52, no. **20**, pp. 12513–12523, 2017.

[35] S. Saki and N. Uzal, *"Preparation and characterization of PSF/PEI/CaCO3 nanocomposite membranes for oil/water separation,"* Environmental Science and Pollution Research, vol. 25, no. **25**, pp. 25315–25326, 2018.

[36] E. Saljoughi, M. Amirilargani, and T. Mohammadi, "Effect of PEG additive and coagulation bath temperature on the morphology, permeability and thermal/chemical stability of asymmetric CA membranes," *Desalination*, vol. 262, no. **1**–**3**, pp. 72–78, 2010,

[37] J. Yin, H. Fan, and J. Zhou, *"Cellulose acetate/poly(vinyl alcohol) and cellulose acetate/crosslinked poly(vinyl alcohol) blend membranes: preparation, characterization, and antifouling properties,"* Desalination and Water Treatment, vol. 57, no. **23**, pp. 10572–10584, 2016.

[38] X. Yu, X. Mi, Z. He, M. Meng, H. Li, and Y. Yan, *"Fouling resistant CA/PVA/TiO2 imprinted membranes for selective recognition and separation salicylic acid from waste water,"* Frontiers in Chemistry, vol. 5, no. JAN, pp. 1–13, 2017.

[39] A. Gao, F. Liu, H. Shi, and L. Xue, *"Controllable transition from finger-like pores to inter-connected pores of PLLA membranes,"* Journal of Membrane Sciences, vol. 478, pp. 96–104, 2015.

[40] X. Yu, Z. Xiong, J. Li, Z. Wu, Y. Wang, and F. Liu, *"Surface PEGylation on PLA membranes via micro-swelling and crosslinking for improved biocompatibility/hemocompatibility,"* RSC Advances, vol. 5, no. **130**, pp. 107949–107956, 2015.

[41] H. Song, F. Ran, H. Fan, X. Niu, L. Kang, and C. Zhao, *"Hemocompatibility and ultrafiltration performance of surface-functionalized polyethersulfone membrane by blending comb-like amphiphilic block copolymer,"* Journal of Membrane Sciences, vol. 471, pp. 319–327, 2014.

[42] Z. Xiong, F. Liu, H. Lin, J. Li, and Y. Wang, *"Covalent Bonding of Heparin on the Crystallized Poly(lactic acid) (PLA) Membrane to Improve Hemocompability via Surface Cross-Linking and Glycidyl Ether Reaction,"* ACS Biomaterial Sciences and Engineering, vol. 2, no. **12**, pp. 2207–2216, 2016.

[43] Y. Raharjo, S. Wafiroh, M. Nayla, V. Yuliana, and M. Z. Fahmi, *"Primary study of cellulose acetate hollow fiber as a green membrane applied to hemodialysis,"* Journal of Chemical Technology and Metallurgy, vol. 52, no. **6**, pp. 1021–1026, 2017.

[44] R. Takai, R. Kurimoto, Y. Nakagawa, Y. Kotsuchibashi, K. Namekawa, and M. Ebara,

"Towards a Rational Design of Zeolite-Polymer Composite Nanofibers for Efficient Adsorption of Creatinine," Journal of Nanomater., vol. 2016, 2016.

[45] S. Mulyati, S. Aprilia, Safiah, Syawaliah, M. A. Armando, and H. Mawardi, *"The effect of poly ethylene glycol additive on the characteristics and performance of cellulose acetate ultrafiltration membrane for removal of Cr(III) from aqueous solution,"* IOP Conference. Series: Material Science Engineering, vol. 352, no. **1**, 2018.

[46] C. Liu *et al.*, *"PMWCNT/PVDF ultrafiltration membranes with enhanced antifouling properties intensified by electric field for efficient blood purification,"* Journal of Membrane Sciences., vol. 576, no. December 2018, pp. 48–58, 2019.

List of Tables

Table 1. Recipe of pristine PSU and modified membranes with phase inversion technique.

Membrane	**PSU (wt%)**	**Sol (mL)**	**PEG (wt%)**	**Sol (mL)**	**CA wt%**	**Sol (mL)**	**Mordenite Zeolite**
PSU	18	-	-	-	-	-	-
PEG/CA-1	18	7	16	4	8	2	0.18
PEG/CA-3	18	7	16	4	8	2	0.48
PEG/CA-5	18	7	16	4	8	2	0.98
PEG-1	18	7	16	4	-	-	0.18
PEG-3	18	7	16	4	-	-	0.48
PEG-5	18	7	16	4	-	-	0.98

Table 2. Comparison of results of Pristine PSU and PSU (with additives).

Membrane materials	BSA rejection (%)	Urea toxins clearance (%)	Creatinine adsorption (μg/gm)	Thrombus formation (%)	Hemolysis ratio (%)	Recalcification time (s)
PSU	N/A	N/A	N/A	N/A	0.55	311
PEG/CA	83	74	9643	4.90	0.37	490
PEG	93	89	7654	5.04	0.46	392

List of Figures

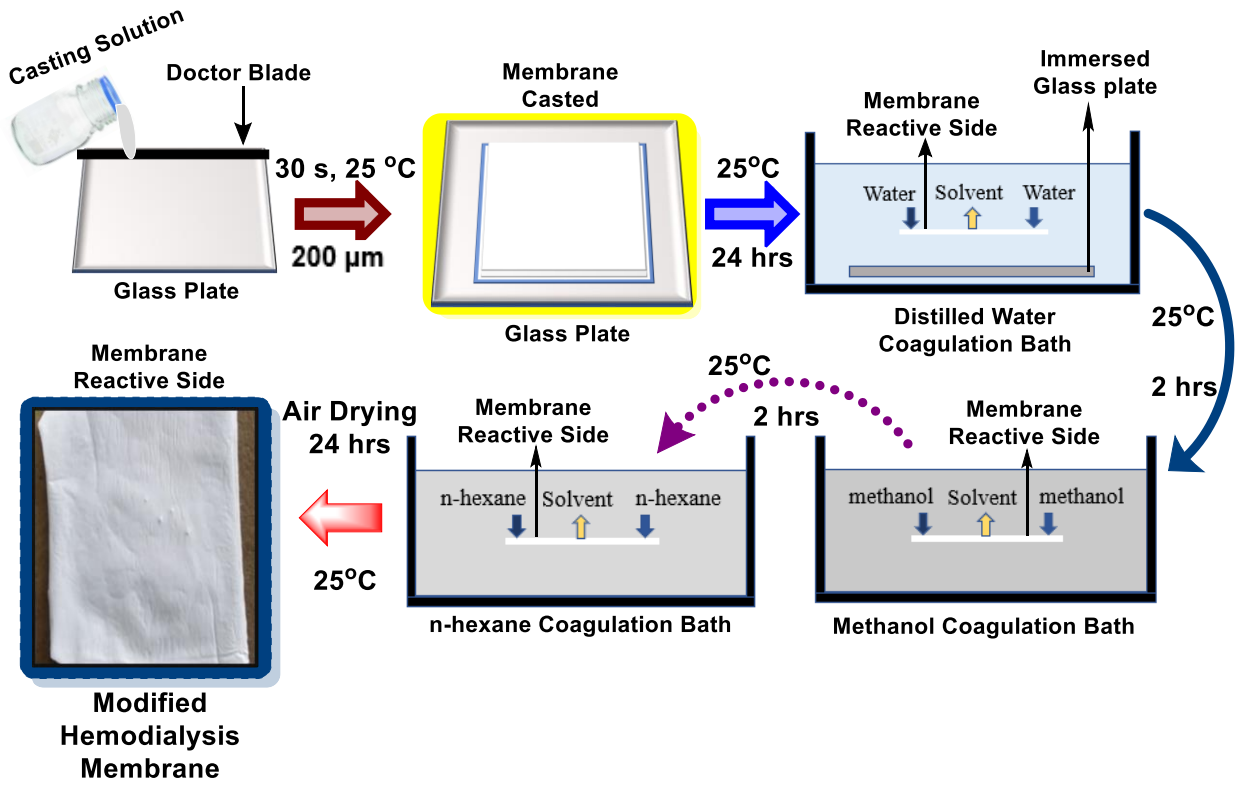

Fig. 1. Fabrication of the membranes by phase inversion technique.

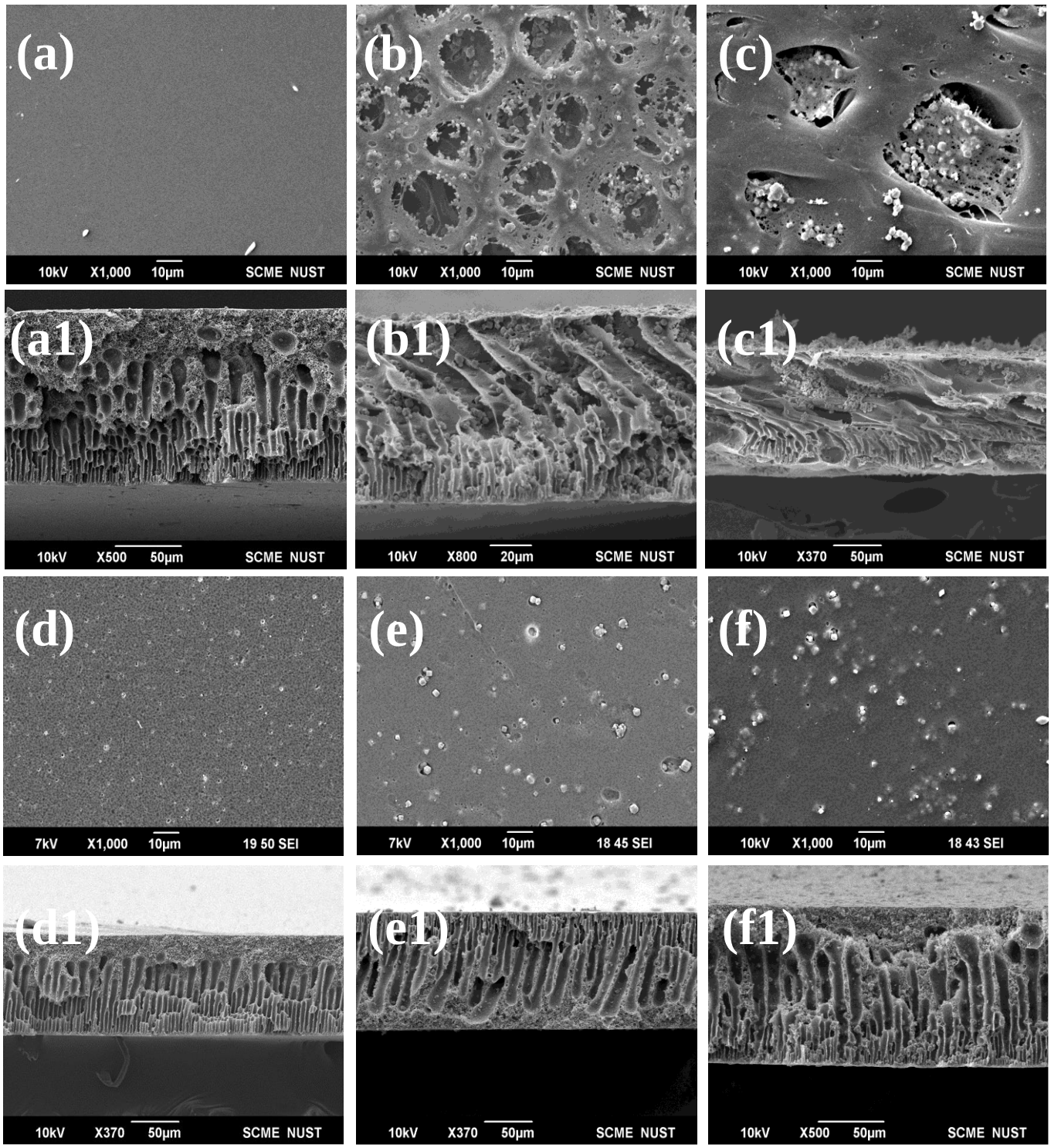

Fig. 2. SEM imaging of the surface (top) and cross-sectional (bottom) morphology of the membranes; (a) PSU (b) PEG/CA-1, (c) PEG/CA-3, (d) PEG-1, (e) PEG-3, (f) PEG-5.

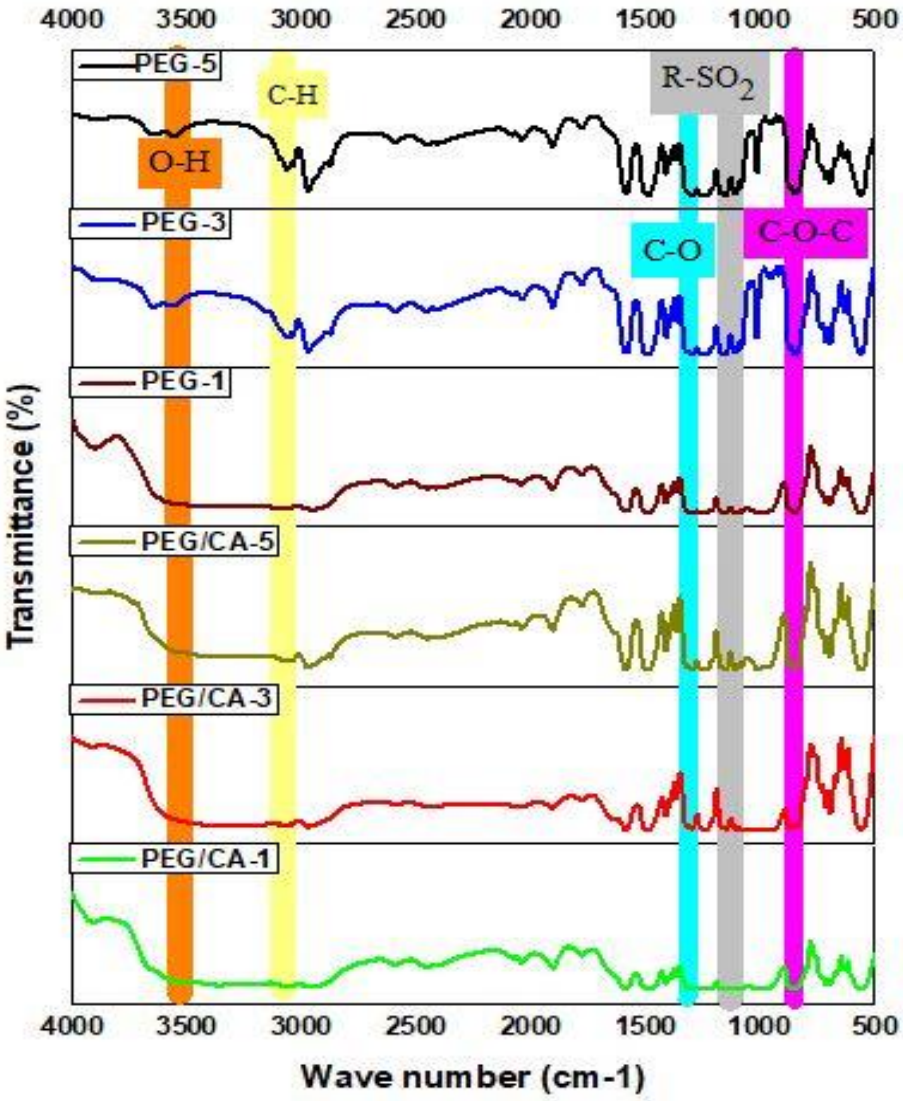

Fig. 3. FT-IR spectrum of modified membranes when PEG and CA, when PEG alone act as an additive**.**

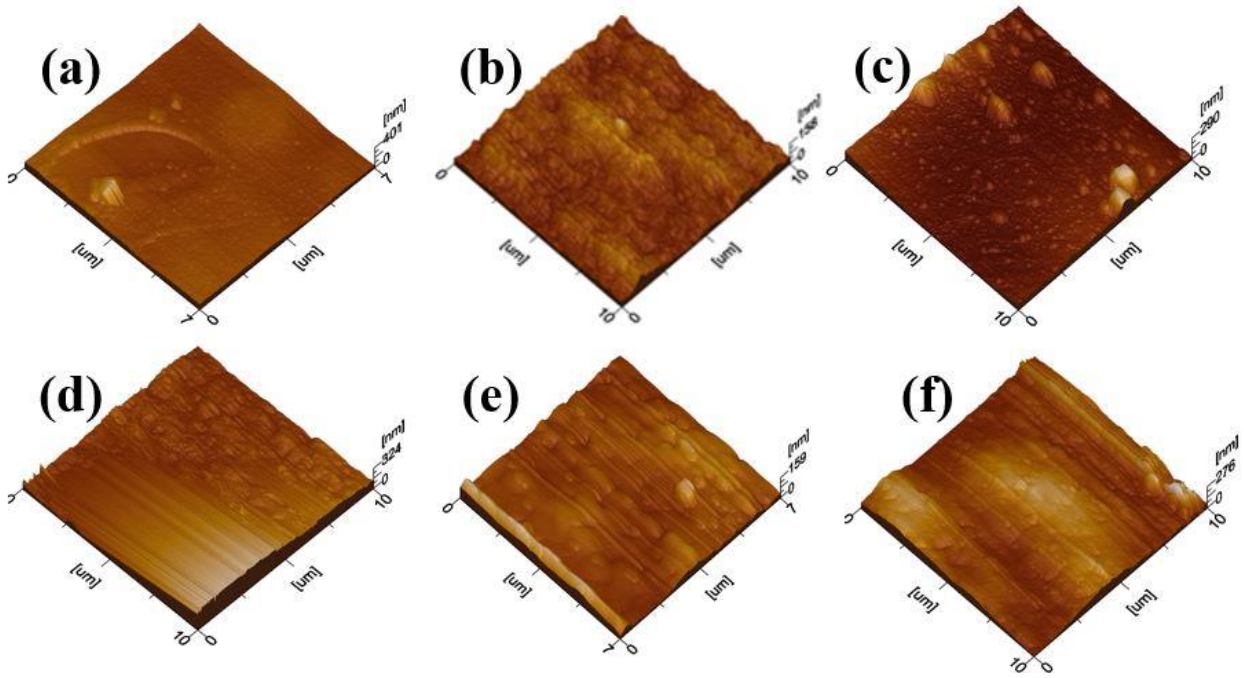

Fig. 4. The AFM imaging to determine the membrane's active layer roughness of pristine PSU and modified membranes; (a) PSU, (b) PEG/CA-1, (c) PEG/CA-3, (d) PEG-1, (e) PEG-3 and (f) PEG-5.

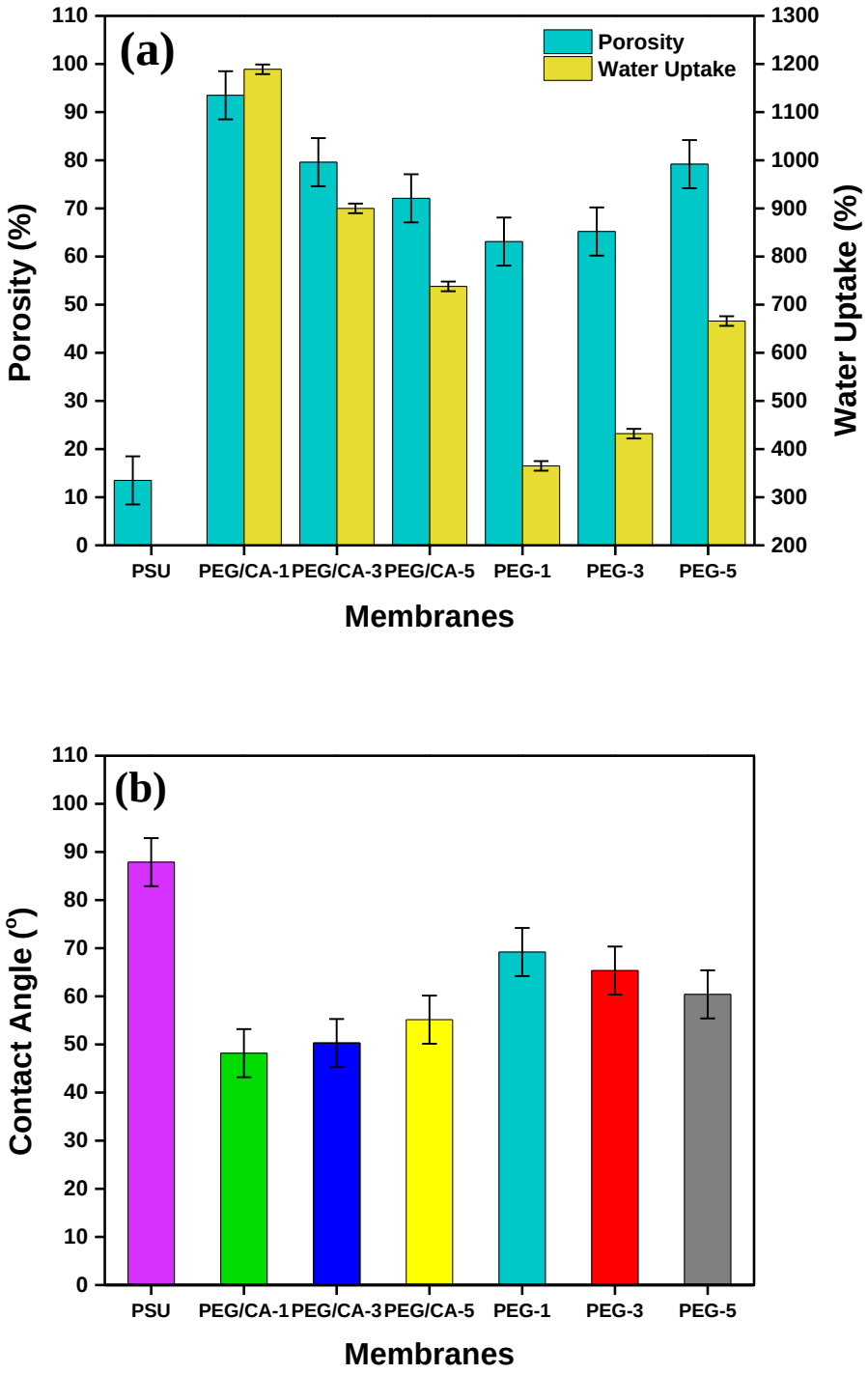

Fig. 5. Measurement of hydrophilicity and hydrophobicity under; (a) The porosity and swelling of the pristine PSU and modified porous membranes after the addition of additives and mordenite zeolite (b) Contact angle measurement of pristine PSU and composite membranes.

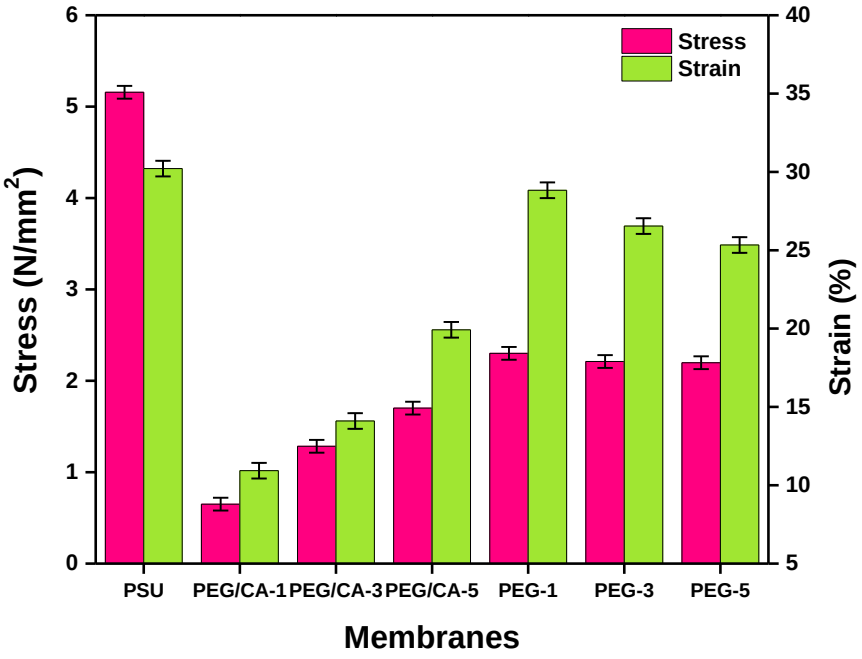

Fig. 6. Stress-strain curve of pristine PSU and modified membranes after the addition of pore-generators along with different concentrations of mordenite zeolite

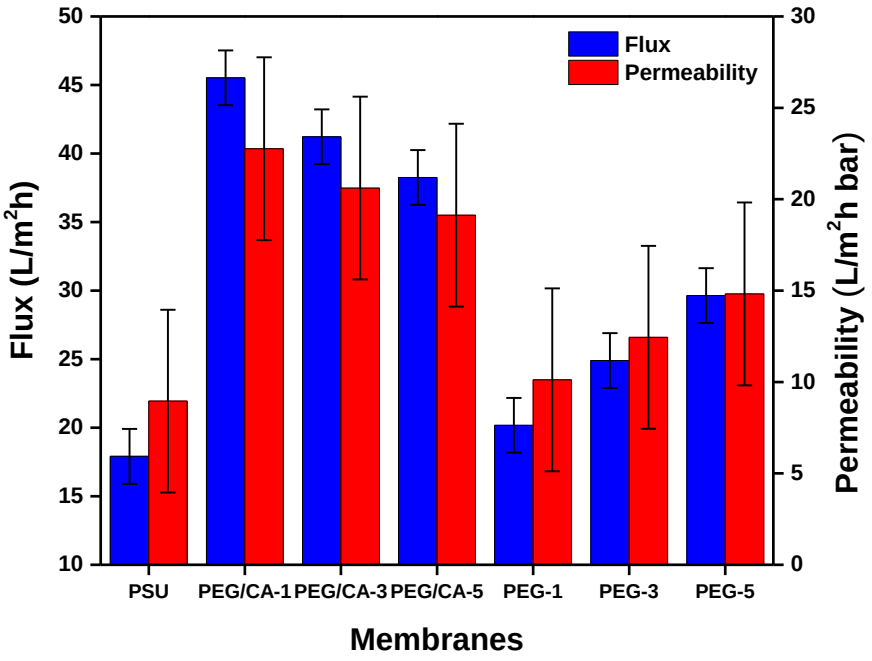

Fig. 7. Water flux and permeability of the membranes when static water was obtained in the permeate in the dead-end filtration cell at (80 minutes).

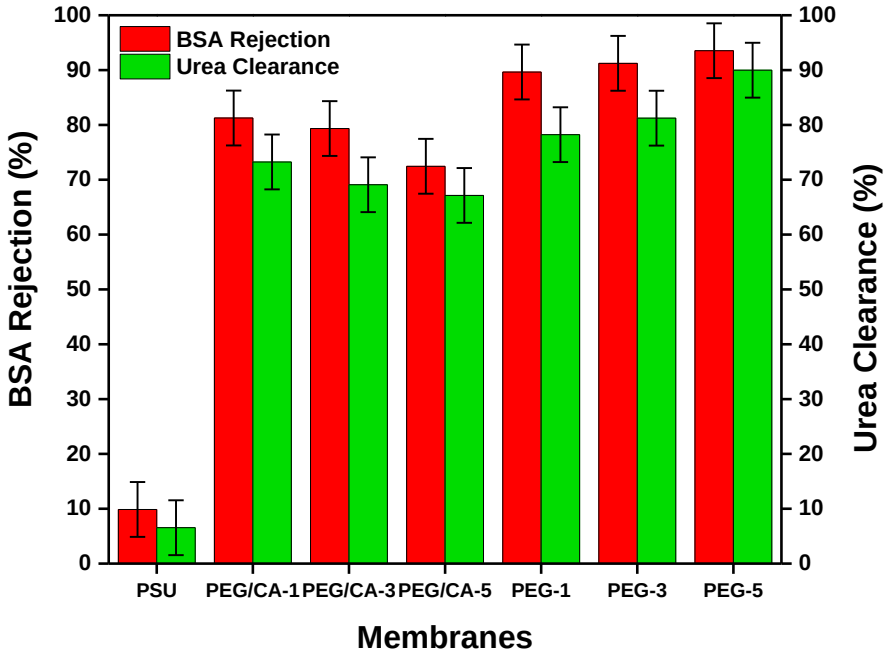

Fig. 8. Urea clearance, BSA rejection of the pristine PSU and modified membranes with different concentrations of mordenite zeolite after 4 hours simulating in dead-end filtration cell.

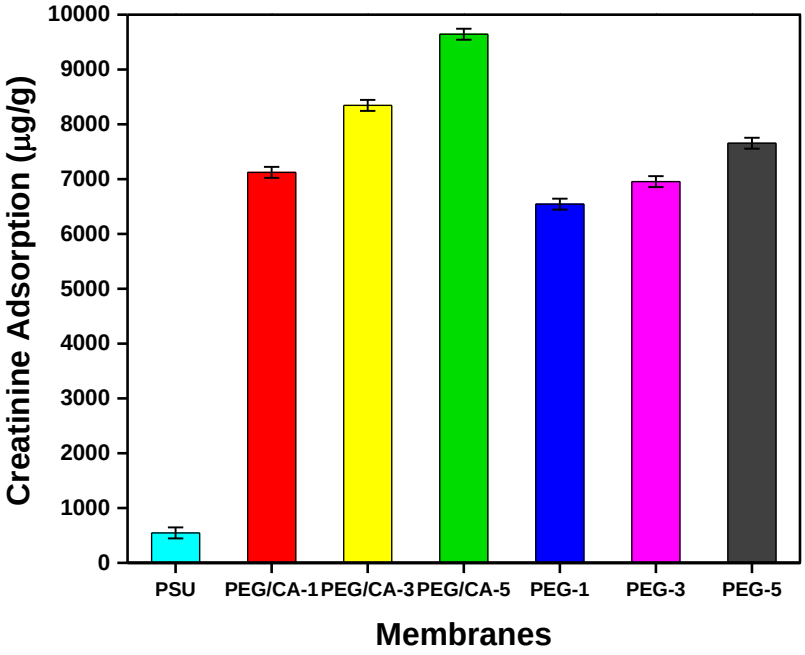

Fig. 9. Comparison of creatinine adsorption capacity of mordenite zeolite in membranes (by membrane mass and by zeolite mass).

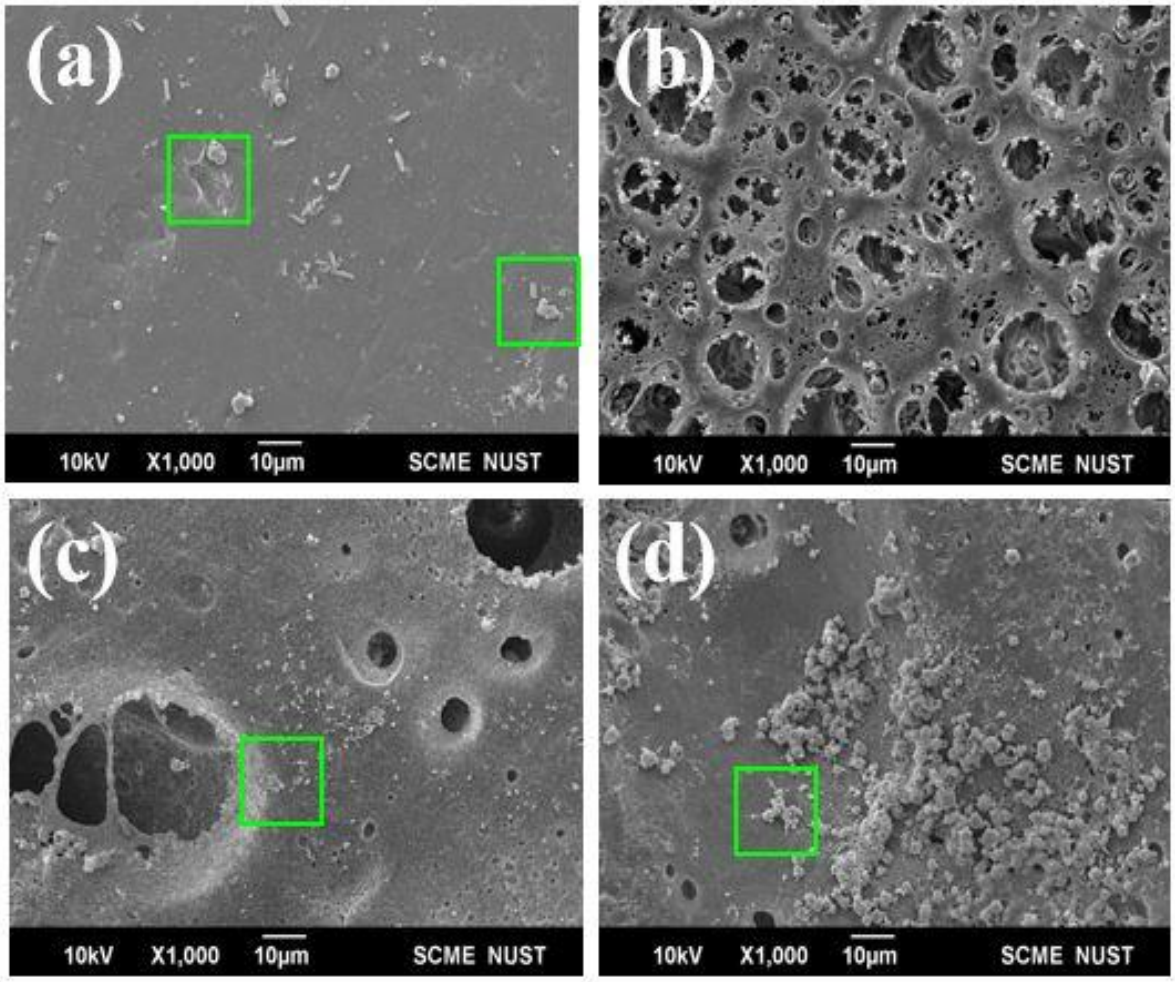

Fig. 10. SEM images of the platelet gathered on pristine PSU and modified membranes; (a) PSU, (b) PEG/CA-1 (No platelet adhesion), (c) PEG-1 and (d) PEG-3.

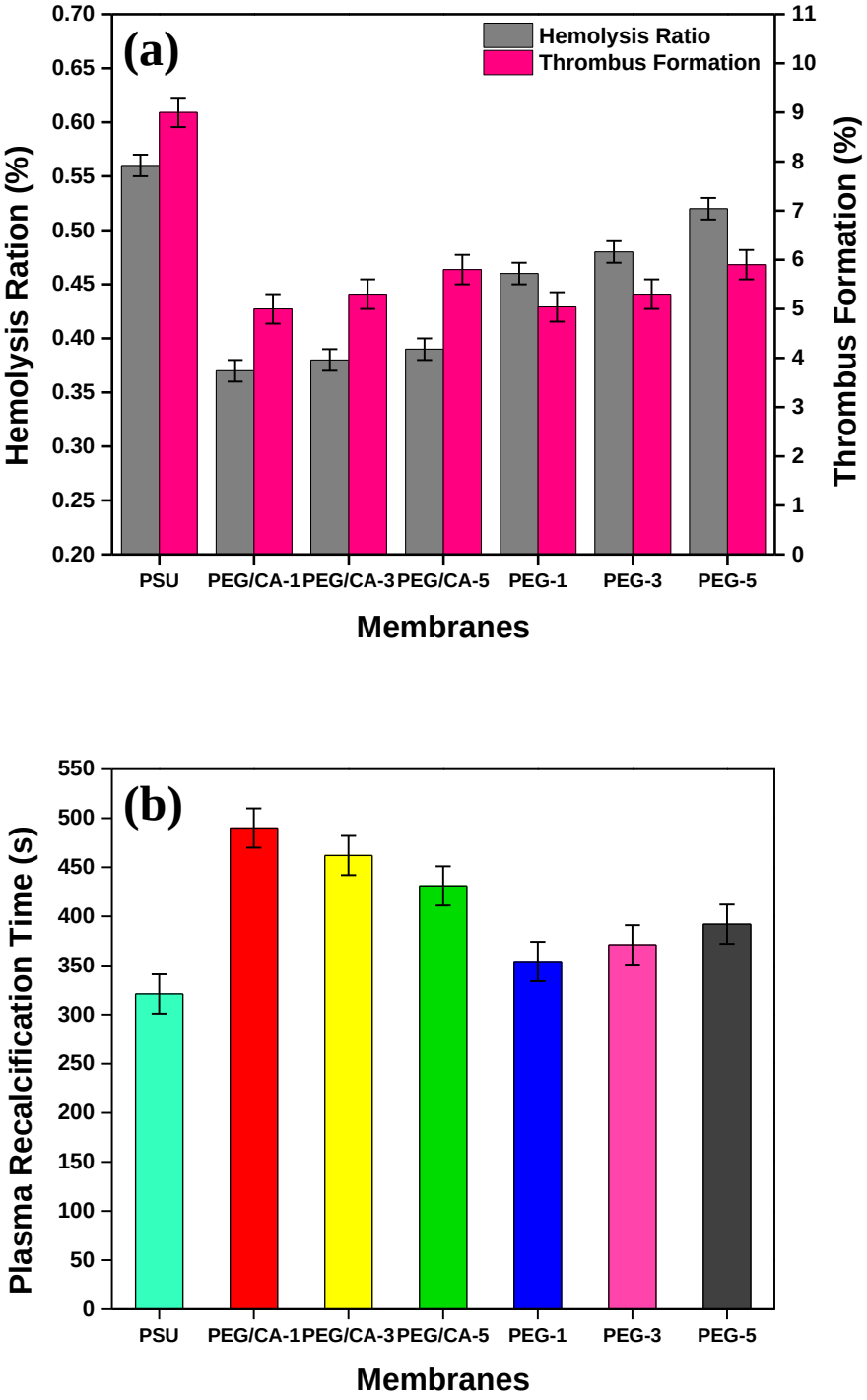

Fig. 11. Hemocompatibility evaluation under; (a) Thrombus formation and Hemolysis ratio of pristine PSU and modified membranes, (b) Improved clotting time of the fabricated membranes with different concentration of mordenite zeolite.